Experimental Eye Research 253 (2025) 110305

Contents lists available at ScienceDirect

Experimental Eye Research

journal homepage: www.elsevier.com/locate/yexer

Research article

Retinal degeneration increases inter-trial variabilities of light-evoked spiking activities in ganglion cells

Da Eun Kim [a,b,1], Sein Kim [a,1], Minju Kim [a], Byoung-Kyong Min [b], Maesoon Im [a,c,d,*]

[a] Brain Science Institute, KIST (Korea Institute of Science and Technology), Seoul, Republic of Korea
[b] Department of Brain and Cognitive Engineering, Korea University, Seoul, Republic of Korea
[c] Division of Bio-Medical Science & Technology, University of Science & Technology, Seoul, Republic of Korea
[d] KHU-KIST Department of Converging Science & Technology, Kyung Hee University, Seoul, Republic of Korea

ARTICLE INFO

Keywords:
Retinal degeneration
Inter-trial spike consistency
Retinal ganglion cells (RGCs)
Electrophysiology

ABSTRACT

Retinal ganglion cells (RGCs) transmit visual information to the brain in the form of spike trains, which form visual perception. The reliabilities of spike timing and count are thought to play a crucial role in generating stable percepts. However, the effect of retinal degeneration on spike reproducibility remains underexplored. In this study, we examined longitudinal changes of both spike timing and count across different RGC types in response to repeated presentations of an identical light stimulus in retinal degeneration 10 (*rd10*) mice (B6.CXBl-*Pde6b*^{rd10}/J), a well-established model of retinitis pigmentosa (RP).

We recorded the spiking responses of RGC populations to repeated white flashes using 256-channel multi-electrode array (MEA) at four *rd10* age groups representing various stages of retinal degeneration. Our experimental results revealed a significant reduction in both spike timing and count consistencies compared to those in wild-type RGC recordings. Furthermore, the inter-trial variability patterns of different RGC types were found to differ throughout the degeneration process. For instance, when the spike time tiling coefficient (STTC) was used to evaluate inter-trial spike timing consistency, contrast-sensitive RGCs (ON, OFF, and ON-OFF types) exhibited a systematic decrease in spike timing consistency as degeneration progressed, whereas the remaining units did not show similar trends. Thus, we concluded that light-evoked spike trains become less consistent as degeneration progresses, with variability in spike timing and spike count varying across cell types.

Given the critical role of spiking reliability in visual perception, our findings highlight the importance of accounting for cell type-specific degeneration patterns and inter-trial spiking inconsistencies when developing visual rehabilitation therapies to achieve enhanced performance. The underlying mechanism(s) driving the inter-trial spiking inconsistencies warrant further investigation.

1. Introduction

The retina is a complex neural circuit that converts light into electrical signals, which are subsequently processed by the brain to create visual perceptions (Fig. 1A). Among the various neuronal classes in the retina, ganglion cells function as the final output neurons, transmitting spiking activities to the brain. Different types of retinal ganglion cells (RGCs) extract distinct visual features from external inputs and convey their unique information to the brain in parallel. These distinctive temporal firing patterns enable each RGC type to encode specific dimensions of visual information, such as contrast and motion, to the cerebral cortex, thereby playing a pivotal role in the comprehensive representation of visual scenes (Wässle, 2004). For example, in vertebrate retinas, ON, OFF, and ON-OFF RGCs detect increases, decreases, and both increases and decreases in luminance, respectively (Roska and Werblin, 2001; Baden et al., 2016). Understanding and decoding the signals from ON and OFF pathways is particularly important because luminance is a fundamental component of visual perception (Schiller, 1995; Schiller et al., 1986; Remington, 2012).

In the context of retinal degeneration, it is essential to evaluate how consistently RGC spiking activities are elicited in response to light stimuli. Extending the concept of the spiking consistency to higher level perception such as object identification, a healthy visual system relies on the repetitive and consistent generation of neural signals on a single

* Corresponding author. Brain Science Institute, KIST (Korea Institute of Science and Technology), 5 Hwarang-ro 14-gil, Seongbuk-gu, Seoul, Republic of Korea.
E-mail address: maesoon.im@kist.re.kr (M. Im).
[1] These authors contributed equally.

https://doi.org/10.1016/j.exer.2025.110305
Received 28 November 2024; Received in revised form 3 February 2025; Accepted 18 February 2025
Available online 19 February 2025

scene to produce a clear visual perception (Livingstone and Hubel, 1987). However, in conditions like retinitis pigmentosa (RP) or age-related macular degeneration (AMD), retinal circuitry is known to be substantially altered as retinal degeneration progresses (Marc and Jones, 2003; Hartong et al., 2006; Jones et al., 2016a, 2016b; Guymer and Campbell, 2023). These changes may lead to inconsistent spiking activities, potentially resulting in confused or unclear perception (Fig. 1B), which was indeed reported in previous clinical studies with RP or AMD patients (Alexander et al., 1995; Arimura et al., 2011; Tejeria, 2002; Wittich et al., 2011). Despite the clinical implication of the spiking inconsistency, no studies have examined the changes in trial-to-trial consistency of RGC spiking activities in response to visual stimuli as a

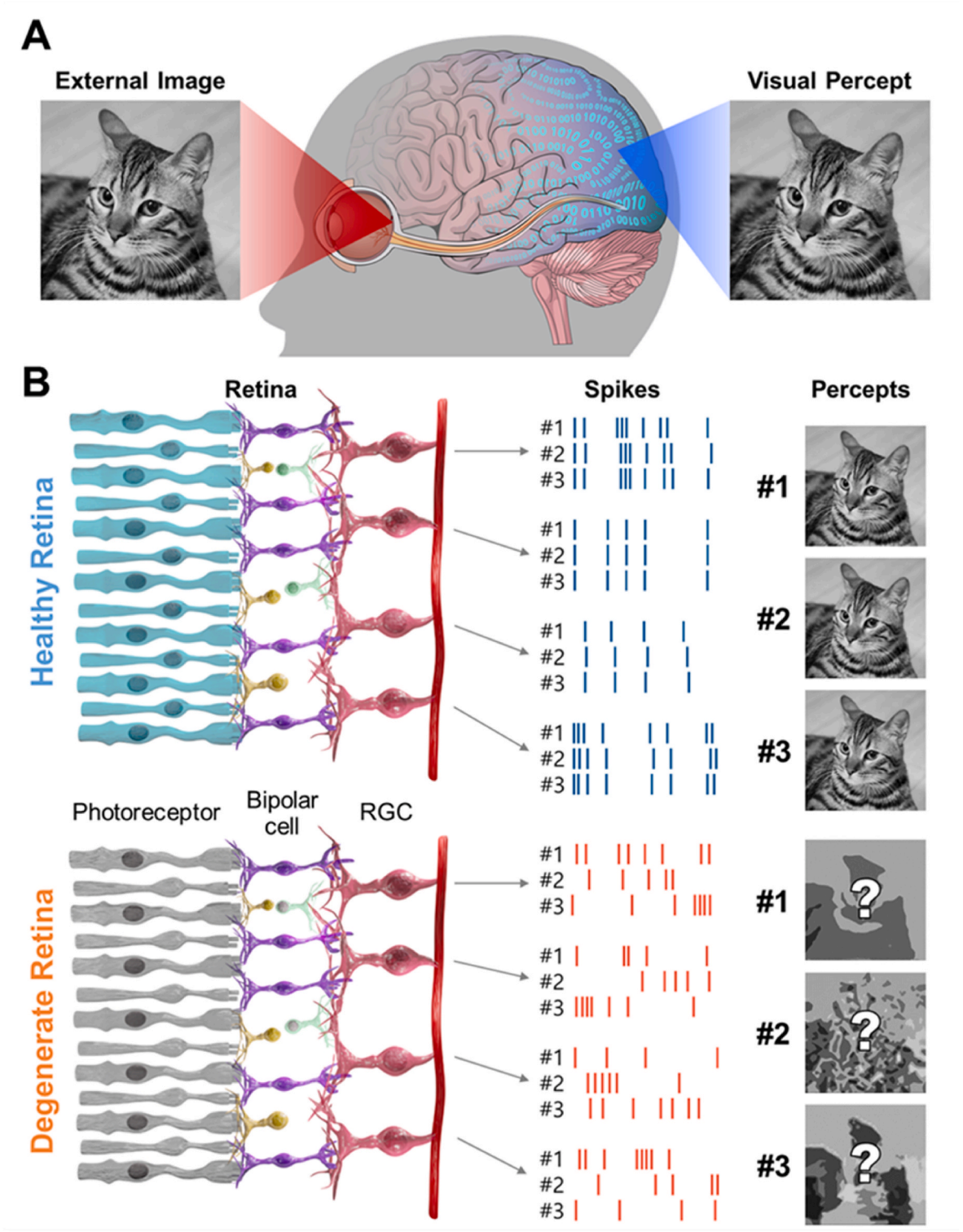

Fig. 1. Schematic illustration of changes in visual percept due to retinal degeneration. **(A)** The imagery percept of external world is built upon the sensory input delivered throughout the visual system, starting from the retina. **(B)** The identification of an object through a healthy visual system is contingent upon the generation of neural signals by a fixed gaze, which in turn creates a visual perception of the object. However, as retinal degeneration takes place and retinal circuitry is destroyed, these signals may become inconsistent, potentially leading to confusion or an unclear perception.

function of retinal degeneration. This can be addressed by analyzing the variability in spike timing and spike count across repeated presentations of the same visual stimulus. Such inter-trial variability offers valuable insights into the stability and reliability of neural coding in degenerating retinas.

Our previous research reported systematic reductions of inter-trial consistency of RGC spiking responses to electrical stimuli over the course of retinal degeneration (Yoon et al., 2020). This work was related to the technological advancement of retinal prostheses, commonly as "*bionic eye*", which aim to elicit visual perception by electrically stimulating the remaining retinal neurons after degeneration. Our findings on electrically-evoked responses suggest that visually-evoked responses may undergo similar alterations during retinal degeneration. Investigating light-evoked responses would be more necessary for deeper understanding of how RP alters natural physiological neural signaling patterns. Unlike electrical stimulation (Yoon et al., 2020), which activates all neuronal classes simultaneously, light stimulation selectively targets photoreceptors, potentially leading to differences in spiking patterns. Comprehensive understanding of spiking characteristics in responses to both stimulation modalities (*i.e.*, electric and light stimulation) must be essential for improved clinical outcomes of retinal prosthetics.

In this study, we investigated the inter-trial variability of RGC spiking activities in response to light stimuli in mouse retinas at various degeneration stages ranging from the early to advanced RP. To analyze a much larger population of RGCs and capture a more comprehensive view of physiological changes as a function of retinal degeneration, we used a multi-electrode array (MEA) system in this work rather than patch-clamp recordings used in our previous work (Yoon et al., 2020). To understand how retinal degeneration affects the consistency of RGC responses, we measured the variability in spike timing and count across repeated presentations of the same visual stimulus. Additionally, we compared the variabilities in spiking activities in ON, OFF, ON-OFF, and non-classified (namely ETC) types of RGCs, expanding from our earlier work reporting only ON and OFF pathways (Yoon et al., 2020). Both the increased sample numbers and the expanded RGC types would offer a more comprehensive view of physiological changes in visual processing as a function of retinal degeneration.

2. Materials and Methods

2.1. Animals

Our animal experiment protocol was approved by the Institutional Animal Care and Use Committee of the KIST (KIST-IACUC-2023-042-6). We used retinal degeneration 10 (*rd10*) mice (B6.CXBl-*Pde6b*^{rd10}/J), a well-established model of RP characterized by a mutation in the *Pde6b* gene. The initial breeding pairs of *rd10* mice were purchased from Jackson Lab (Bar Harbor, ME, USA) and a colony has since been maintained at the KIST animal facility.

In our study, *rd10* mice were sacrificed at four distinct ages to represent different stages of retinal degeneration (Yoon et al., 2020): postnatal days (P) 15 ± 1 (3 animals), P20 ± 1 (3 animals), P30 ± 1 (4 animals), and P60 ± 1 (3 animals). These time points were chosen to reflect the progression of degeneration, spanning from early to advanced stages: before degeneration onset (P15), around the onset of rod degeneration (P19), following the onset of dendritic retraction in rod bipolar cells (P30), and an advanced stage with minimal visual responses to light stimulus (P60) stages (Barhoum et al., 2008; Biswas et al., 2014; Cha et al., 2022; Gargini et al., 2007; Piano et al., 2013). Additionally, wild type (*wt*) mice (C57BL/6J) at P56 ± 7 (5 animals) were used as a control group to provide baseline data for comparison.

2.2. Retinal tissue preparation and electrophysiological recording

Ex vivo electrophysiological recordings of RGC spikes were performed using a 256-channel multi-electrode array (MEA; 256MEA100/30iR-ITO, Multi Channel Systems GmbH, Reutlingen, Germany). After euthanasia, eyeballs were carefully enucleated and dissected, and a retina was placed ganglion cell side down on the MEA. The retina tissue was continuously superfused with oxygenated artificial cerebrospinal fluid (ACSF) at a flow rate of approximately 0.8 mL/min, and the solution temperature was maintained at 32–34 °C to preserve physiological conditions during the recordings.

RGC spiking activities were recorded using the MEA mounted on a custom interface printed circuit board (PCB) equipped with 256 pogo pins for electrical interconnection. Spiking signals were amplified by four 64-channel amplifiers (RHD2164, Intan Technologies, Los Angeles, CA, USA). We used an RHD 512-channel recording controller and RHX data acquisition software (Intan Technologies). The preparation of retinal samples and the electrophysiological recordings were conducted under red illumination.

2.3. Visual stimulation

Visual stimuli were generated and controlled using custom software and delivered via a digital micromirror device (DMD) projector (DLP3010, Texas Instruments, Dallas, TX, USA) as illustrated in Fig. 2. White spots with a radius of 15.6 mm, which was large enough to cover all recording electrodes of MEA, were presented for 1 s on a uniform black background. Each stimulus was followed by a 2-s-long full-field black background to prevent adaptation and ensure recovery. For trial-to-trial variability assessment of spiking activities arising in RGCs, each visual stimulus was repeated at least 10 times.

2.4. Spike sorting and RGC type classification

The recorded electrophysiological signals were processed using custom Python software: SpikeInterface (Buccino et al., 2020) was employed as a platform module and SpyKING CIRCUS algorithm was utilized for spike sorting (Yger et al., 2018).

We classified RGCs based on firing rates computed in specific four time periods. To compare the firing rate in different time intervals, we computed mean firing rate (MFR) for four cases: A_1, A_2, A_3, and A_4. A_1 represents the MFR during the first 500 msec after the onset of the light stimulus, while A_2 refers to the MFR during the first 500 msec after the offset of the light stimulus. Similarly, A_3 represents the MFR during the 500 msec before the onset of the light stimulus, and A_4 represents the MFR during the 500 msec before the offset of the light stimulus. Units that did not strongly respond to the light stimuli, if neither $A_1 > A_3$ nor $A_2 > A_4$, were grouped as ETC RGCs, which we categorized as a separate type in our study. Identification of ETC cells enhances the accuracy of RGC type classification because RGCs showing weak visually-evoked responses were filtered beforehand, a category distinct from ON, OFF, or ON-OFF types (without further identifying a specific RGC subtype), which will be explained later. This classification of ETC cells is an arbitrary grouping introduced in our study to include as many light-responsive RGCs as possible after filtering out those with weak visually-evoked responses beforehand.

After the identification of ETC RGCs, light responsive RGCs were classified into three types based on their firing pattern evoked by light stimuli: ON, OFF, and ON-OFF types. Classification was determined using a bias index (Carcieri et al., 2003), which can be calculated by the following equation:

$$\text{Bias index} = \frac{A_1 - A_2}{A_1 + A_2}$$

Units with a bias index greater than 0.3 were classified as ON RGCs, while units with a bias index less than −0.3 were classified as OFF RGCs, given that the light stimulus was a bright full-field spot flash. Units with a bias index within the range of [−0.3 0.3] were classified as ON-OFF RGCs. To ensure the reliability of the data, we excluded units with an

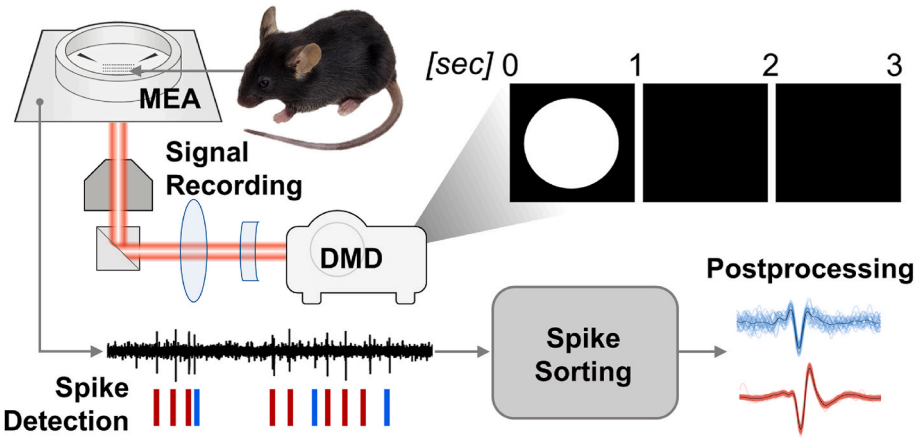

Fig. 2. Visualization of the experimental method. Following the placement of the mouse retinal tissue on the multi-electrode array (MEA) electrode, a repetition of full-field spot light stimuli was presented using digital micromirror device (DMD). Recorded signals were subsequently processed and analyzed in order to separate them into the firing pattern of individual cells.

MFR in the bottom 20% from the analysis. The final numbers of RGCs we included in our analyses were 24 ON, 12 OFF, 20 ON-OFF, and 193 ETC cells from *wt* mice, 54 ON, 7 OFF, 10 ON-OFF, and 465 ETC cells for *rd10* P15 mice, 79 ON, 34 OFF, 17 ON-OFF, and 371 ETC cells for *rd10* P20 mice, 370 ON, 104 OFF, 166 ON-OFF, and 571 ETC cells for *rd10* P30 mice, 50 ON, 19 OFF, 70 ON-OFF, and 151 ETC cells for *rd10* P60 mice, respectively. The classification resulted in a significant proportion of ETC cells, as the full-field stimulation approach utilized as a simplified stimulus framework inherently lacks the capacity to evoke optimal responses from various RGC types (*see* **Discussion**).

The proportion of ETC cells was decreased at the advanced stages of retinal degeneration. It is likely to be due to two key factors. First, as degeneration progresses, the absolute number of photoreceptors decreases, leading to a general reduction in overall spiking activity across RGCs (Barhoum et al., 2008). Second, during data processing, we applied a firing rate threshold as part of our curation process, excluding cells that exhibited activity below a certain criterion. This exclusion criterion inevitably results in a higher number of low-firing cells being filtered out, thereby affecting the final proportion of ETC cells included in the analysis.

2.5. Spike time tiling coefficient (STTC)

To assess variability in spiking activity, we computed three metrics: the spike time tiling coefficient (STTC), van Rossum distance (D_{vR}), and Fano factor (FF). The first two metrics were calculated for every pair of trials, while the FF was computed across every trial. For all metrics, we used spiking activities recorded for 2 s including 1 s of the light stimulus itself and 500 msec before/after the light stimulus.

STTC is a reliable metric for assessing spike timing correlations between two spike trains, offering valuable insights into temporal similarity. Unlike the traditional correlation index, the STTC is not influenced by firing rate, accurately distinguishes between lack of correlation and anti-correlation, and excludes periods of silence from contributing to the correlation measure (Cutts and Eglen, 2014). It is calculated as a pairwise correlation between two spike trains, A and B, using the following equation:

$$\mathrm{STTC} = \frac{1}{2}\left(\frac{P_A - T_B}{1 - P_A T_B} + \frac{P_B - T_A}{1 - P_B T_A}\right)$$

where P_A denotes the ratio of spikes from train A that occur within a specified temporal interval (Δt) of any given spike from train B (with P_B computed similarly), T_A denotes the fraction of the entire recording duration that aligns within $\pm$ Δt of any spike from train A (with T_B calculated in a similar manner). An STTC value close to 1 indicates a high degree of temporal correlation between the two spike trains. We used Δt of 100 msec in this work.

2.6. van rossum distance (D_{vR})

In addition to STTC, we computed van Rossum distance (D_{vR}) to analyze spike inconsistencies at both macro and micro levels. While both STTC and D_{vR} utilize spike timing information, they have distinct characteristics that make each metric uniquely valuable for different aspects of analysis. For example, STTC is more suitable for evaluating broader synchrony and pattern correlations (Nirenberg and Latham, 2003) whereas D_{vR} excels in analyzing fine temporal coding by capturing precise temporal differences in spike timing and is robust to minor fluctuations (Satuvuori and Kreuz, 2018). In detail, the D_{vR} quantifies the dissimilarity between spike trains by capturing both causal nature of spike train and differences in spike timing and firing patterns (van Rossum, 2001). D_{vR} transforms two discrete spike events into continuous functions by convolving each spike with an exponential filter $H(t)\exp(-t/t_c)$, which implements biologically plausible temporal decay. Here, t_c is the time constant and $H(t)$ is a Heaviside step function. The squared difference, or Euclidean distance, between the convolved representation from two spike trains is then integrated over time. Using the resulting continuous functions $\tilde{x}(t)$ and $\tilde{y}(t)$, D_{vR} is calculated as follows:

$$D_{vR} = \sqrt{\frac{1}{\tau_R}\int_0^\infty |\tilde{x}(t) - \tilde{y}(t)|^2 dt}$$

A larger the D_{vR} value indicates greater inconsistency between the two spike trains. In our study, we used 500 msec for the value of t_c. However, D_{vR} is known to lack robustness to recording duration. This limitation was deemed negligible in our study, as the maximum recording duration was 90 s, which falls well below the minimum value identified as problematic in previous analysis (Cutts and Eglen, 2014).

2.7. Fano factor (FF)

We employed FF analysis to quantify the inter-trial variability in the number of RGC spikes: FF is the ratio of spike count variance to its mean, providing a normalized metric for assessing spike count variability (Kara et al., 2000; Uzzell and Chichilnisky, 2004). As FF is defined as the variance over the mean of spike count $(N_{\Delta t})$ within Δt, it can be expressed by the following formula:

$$FF = \frac{var(N_{\Delta t})}{mean(N_{\Delta t})}$$

In our study, we used a time bin (Δt) of 500 msec after the onset or offset of the light stimulus, depending on the classified type of each cell. For ON-OFF and ETC cells, FFs were calculated for both periods (*i.e.*, 500 msec after the onset/offset of the light stimulus) and averaged. An FF of 1 indicates that the variance equals the mean, characterizing a Poisson process where events occur independently at a uniform rate; in our context, spiking is entirely stochastic (or random). An FF greater than 1 indicates increased variability compared to a Poisson process, suggesting irregular spiking patterns that may result from factors such as synaptic noise or the absence of refractory period (Gabbiani and Cox, 2017), as observed in degenerate tissue (Yoon et al., 2020). Conversely, an FF below 1 indicates reduced variability, suggesting more regular or predictable spiking, typically observed in controlled or highly structured neural firing patterns.

2.8. Statistical significance

Statistical significance was tested to compare abovementioned variability metrics (*i.e.*, STTC, D_{vR}, and FF) across different stages of retinal degeneration as well as between the ON and OFF pathways. Data from the four age groups of *rd10* mice (P15, P20, P30, and P60) were compared to a *wt* control group to systematically track any alterations in inter-trial spiking consistencies as degeneration progressed.

Data are expressed as the mean with the interquartile range. A one-way ANOVA was performed, followed by Tukey's HSD post-hoc tests, with *p*-values below 0.05 considered statistically significant ($^*p < 0.05$; $^{**}p < 0.01$; $^{***}p < 0.001$).

3. Results

3.1. Retinal degeneration diminishes the distinctive response patterns of each RGC types

It is well known that, in a healthy retina, each type of RGC exhibits a unique spiking pattern in response to visual stimuli (Baden et al., 2016; Cowan et al., 2020). For instance, ON cells exhibit robust firing at the onset of a bright light stimulus, while OFF cells respond with increased spiking at the offset of a bright light stimulus (or the onset of a dark light stimulus). On the other hand, ON-OFF cells display a dual response, firing at both the onset and the offset of light, reflecting their capability to detect luminance changes in both directions.

To visualize how abovementioned characteristic responses patterns are altered as a function of degeneration level, we show raster plots and peristimulus time histograms (PSTHs) of five representative RGCs from each type recorded from *wt* and *rd10* mice (Fig. 3). In the three contrast-

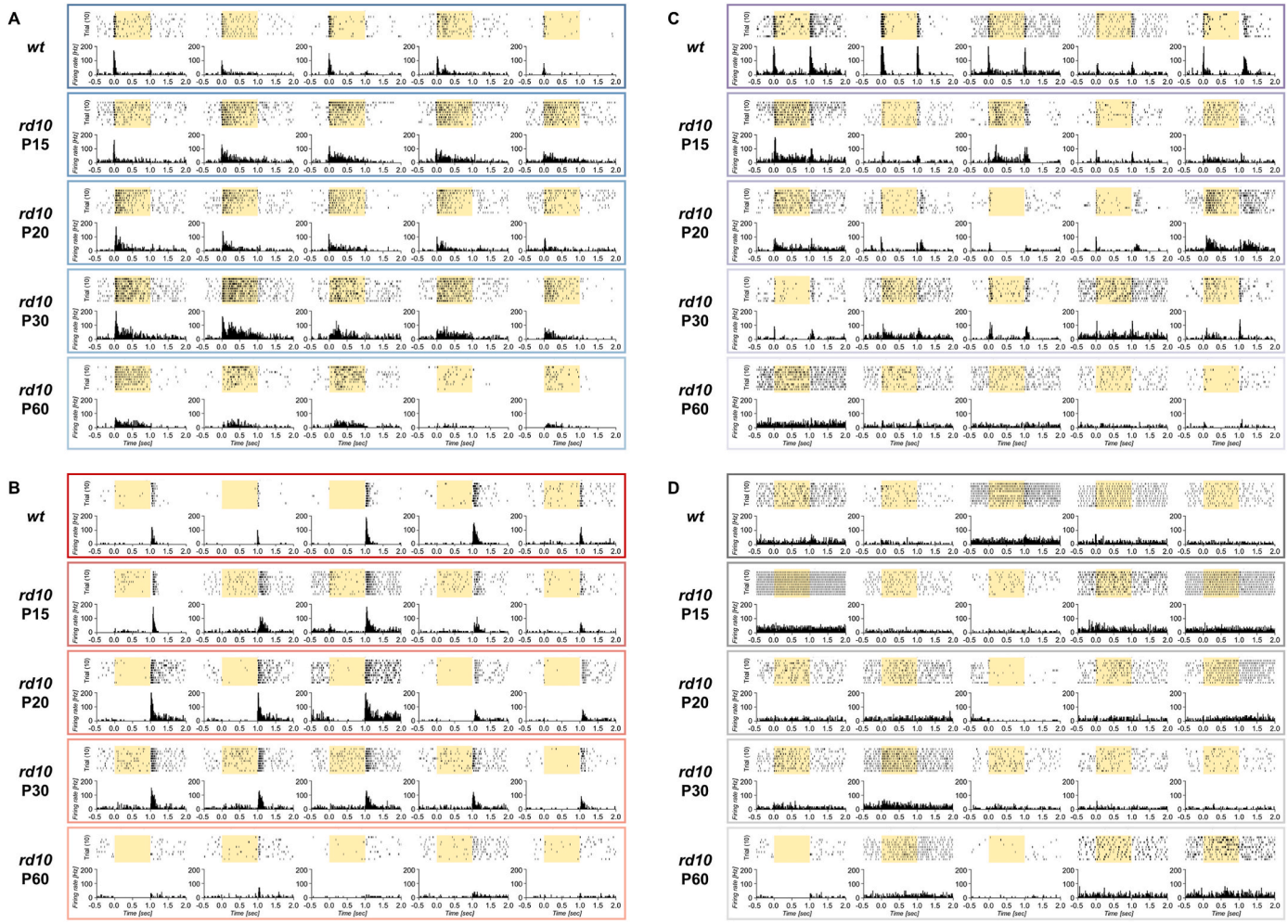

Fig. 3. Firing patterns of 5 representative RGCs in each type. Each panel refers to **(A)** ON, **(B)** OFF, **(C)** ON-OFF, and **(D)** ETC types. Each row in a colored box illustrates raster plots and peristimulus time histogram (PSTHs) of the cells from same age group. For each segment, the upper is a raster plot for 10 repeated light stimuli, and the lower is a PSTH of those trials. In each raster plot, a yellow band indicates the duration of light stimulus. (For interpretation of the references to color in this figure legend, the reader is referred to the Web version of this article.)

sensitive RGC types (ON, OFF, and ON-OFF) of healthy retinas, distinct and consistent spiking patterns were evident following the onset and/or offset of light stimuli (Fig. 3A-3C). However, as degeneration progressed, these patterns became increasingly disorganized, with reduced spike precision and more variable response timing across trials. For example, in ON cells (Fig. 3A), raster plots from *wt* retinas exhibited well-aligned spike trains across repeated stimuli, visualized in the PSTHs as sharp, phase-locked activity immediately after light onset (first row, Fig. 3A). In *rd10* mice, as degeneration advanced, these sharp peaks broadened and became less distinct (second through fifth rows, Fig. 3A), reflecting a loss of firing precision characteristic of this RGC type. Similar degradation was observed in OFF cells following light offset (Fig. 3B) and in ON-OFF cells after both light onset and offset (Fig. 3C). In contrast, ETC cells, which were classified as lacking significant light-

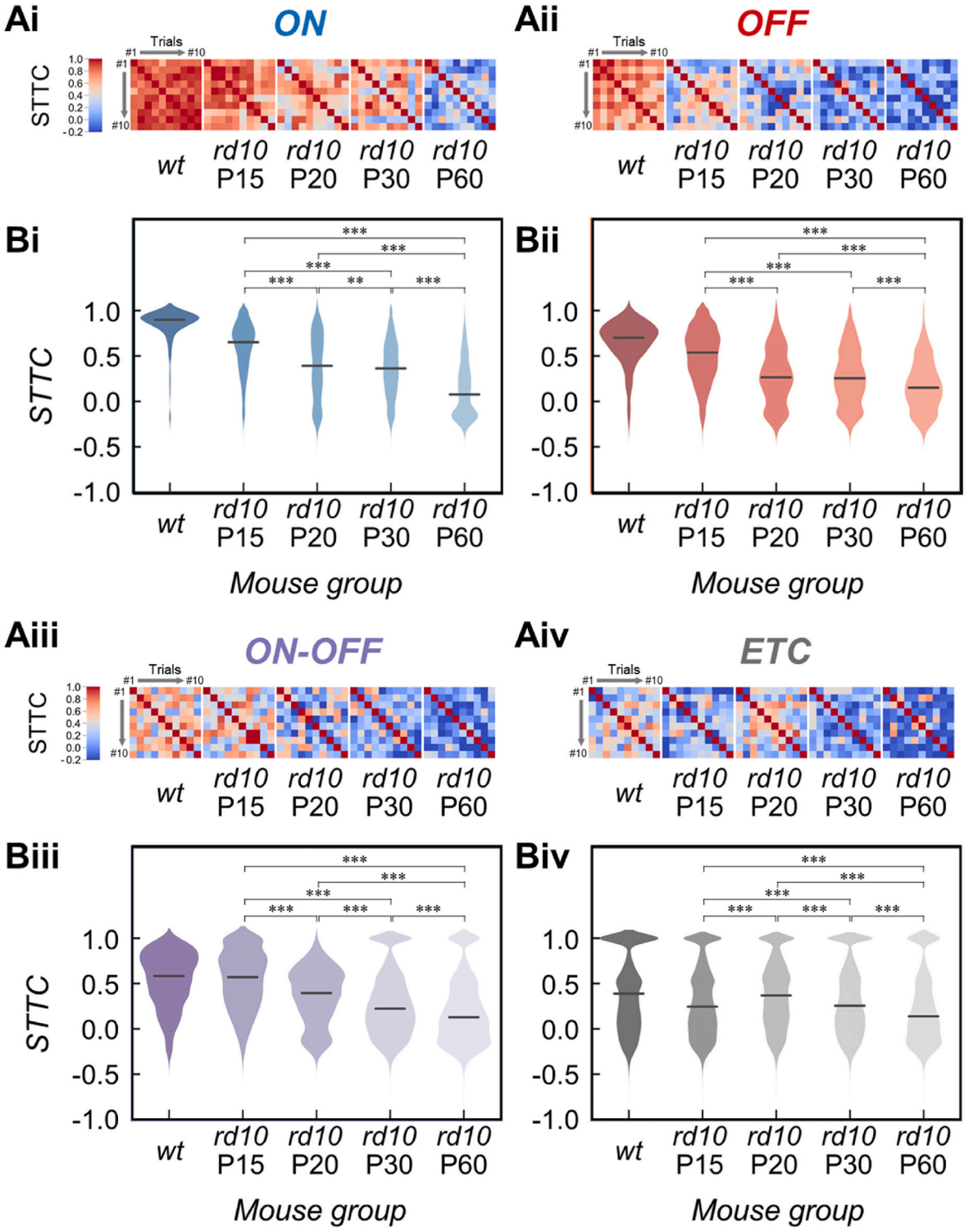

Fig. 4. STTC analysis reveals systematic reduction of inter-trial correlation consistency in spike timings. (**A**) Heatmaps of a representative ON (Ai), OFF (Aii), ON-OFF (Aiii) and ETC cells (Aiv) in *wt* and each age group or *rd10*. (**B**) Violin plots of every STTC values of each trial in ON (Bi), OFF (Bii), ON-OFF (Biii) and ETC cells (Biv). Each STTC data point was omitted in each violin plot for brevity. Black horizontal lines in the middle of the violin plot represent $STTC_{AVG}$.

triggered activity, displayed no aligned spike trains in either raster plots or PSTHs, even in healthy retinas, and continued to exhibit no discernible patterns throughout the degeneration (Fig. 3D). This degradation in the temporal properties of light-responsive RGC spikes (*i.e.*, spiking activities of ON, OFF, and ON-OFF types) reflects the impact of degeneration on the functional characteristics of their retinal circuitries.

3.2. Retinal degeneration elevates trial-to-trial variability in spike timing

Consistent with our previous study (Yoon et al., 2020), retinal degeneration showed a systematic decrease in trial-to-trial consistencies of spiking activities in all metrics we tested (*i.e.*, STTC, D_{vR}, and FF). First, the average values of STTC ($STTC_{AVG}$) systematically decreased in all but ETC types (*i.e.*, ON, OFF, and ON-OFF cells) as degeneration progressed (Fig. 4). STTC heatmaps were generated using data from 10 repeated trials of a representative cell that closely matched the $STTC_{AVG}$ across all classified cells within each group. In ON (Fig. 4Ai) and OFF (Fig. 4Aii) cells, the heatmaps showed a consistent color shift from red to blue, indicating reduced levels of spike timing correlation across trials in a given cell. For ON cells, our population-level analysis revealed a significant decrease in $STTC_{AVG}$ across degeneration stages (0.85 ± 0.19, 0.59 ± 0.28, 0.37 ± 0.36, 0.35 ± 0.31, and 0.13 ± 0.3 for *wt*, *rd10* P15, P20, P30, and P60, respectively; Fig. 4Bi). Notably, every pairwise comparison between the *rd10* age groups yielded statistically significant differences ($p < 0.05$). Likewise, representative OFF cells also showed a systematic color change in their STTC heatmaps throughout the progression of retinal degeneration (Fig. 4Aii). $STTC_{AVG}$ values of the OFF cells also exhibited a similar decrease with advancing degeneration (0.65 ± 0.24, 0.51 ± 0.29, 0.27 ± 0.31, 0.27 ± 0.31, and 0.18 ± 0.28; Fig. 4Bii). Violin plots of $STTC_{AVG}$ for OFF cells revealed that P15 cells showed the highest $STTC_{AVG}$ among all age groups of *rd10*, while P60 showed the lowest. The result also highlighted that *rd10* P20 cells resembled P30 cells more closely than P15 cells, which was interesting compared to our previous work using electric stimulus (Yoon et al., 2020). In the case of electrically-stimulated retina, $STTC_{AVG}$ values for OFF cells in *rd10* showed no statistically significant difference between P15 and P19 ($p > 0.05$) but demonstrated a dramatic decrease by P31. On the contrary, for ON cells, the $STTC_{AVG}$ values have exhibited a similar downward trend with a dropping value at a comparable degeneration stage compared to the previous work (Yoon et al., 2020). The disparity of $STTC_{AVG}$ changing patterns between light and electric stimulation suggests that robustness in spike timing consistency lasts differently during retinal degeneration depending on the stimulation modality, likely reflecting differences in the rate of structural and electrophysiological degradation within retinal circuits as degeneration progresses (Gargini et al., 2007). Gargini et al. reported physiological changes in the inner retina as early as P18, preceding any noticeable morphological alterations in inner neurons; which can trigger different tendencies of firing patterns depending on how directly the modality is stimulating the retinal neurons. It is also noteworthy that, in *wt* retinas, $STTC_{AVG}$ values were significantly higher in ON cells compared to other RGC types, highlighting differential degradation of spike timing variabilities between ON and OFF pathways (Fig. 4Bi, *see* **Discussion**).

ON-OFF cells also displayed a systematic reduction in $STTC_{AVG}$ values (0.54 ± 0.31, 0.54 ± 0.32, 0.36 ± 0.31, 0.28 ± 0.36, and 0.2 ± 0.37; Fig. 4Biii). Compared to ON or OFF cells, ON-OFF cells displayed a more pronounced shift toward blue in their STTC heatmaps (Fig. 4Aiii). In contrast, ETC cells showed no clear trend in $STTC_{AVG}$ values across degeneration stages (0.41 ± 0.42, 0.31 ± 0.39, 0.38 ± 0.37, 0.32 ± 0.39, and 0.23 ± 0.4; Fig. 4Biv). The heatmaps of ETC cells showed only subtle color changes, with no apparent correlation with the progression of retinal degeneration (Fig. 4Aiv). The lack of any clear trend in ETC cells is likely due to the heterogeneous nature of this group, which may comprise multiple cell types with varied characteristics (*see* **Discussion**). Interestingly, ON-OFF and ETC cells exhibited a considerable portion of pairwise comparisons with an STTC value of nearly 1 (Fig. 4BiiiBiii and 4Biv). In contrast, ON and OFF cells showed no noticeable clustering near an STTC value of 1 (Fig. 4Bi and 4Bii). These clustering in ON-OFF and ETC cells is likely driven by trials with consistently high firing rates (*e.g.*, see the leftmost raster plot of *rd10* P15 in Fig. 3C and 3D), where spontaneous spiking activity associated with retinal degeneration appears to dominate.

We also computed van Rossum distance (D_{vR}) to examine the variability in the precise timing of spikes across pairs of trials, offering a finer temporal resolution compared to STTC analysis (Satuvuori and Kreuz, 2018). Regardless of RGC type, our analyses revealed an increase in the average of D_{vR} ($D_{vR,AVG}$) from early (*rd10* P15) to advanced (*rd10* P60) stages of degeneration, suggesting increased variability of spike timing. In detail, ON cells exhibited an overall increasing trend with some fluctuations in $D_{vR,AVG}$ (3.95 ± 2.15, 5.12 ± 3.28, 4.57 ± 3.75, 6.19 ± 4.13, and 5.25 ± 3.95 for *wt*, *rd10* P15, P20, P30, and P60, respectively; Fig. 5A). OFF cells showed a similar pattern with incremental changes in $D_{vR,AVG}$ over the progression of degeneration (3.67 ± 2.14, 4.3 ± 2.19, 4.02 ± 2.5, 5.29 ± 2.91, and 5.07 ± 2.67; Fig. 5B). Contrary to ON or OFF cells, ON-OFF cells demonstrated relatively steady incremental changes in $D_{vR,AVG}$ except the drop in P60 cells (6.93 ± 3.27, 4.59 ± 2.79, 5.95 ± 4.49, 6.48 ± 3.84, and 5.76 ± 3.86; Fig. 5C). On the other hands, ETC cells showed almost monotonous rise across *rd10* age groups, occurring in a relatively predictable manner (7.09 ± 5.13, 6.18 ± 5.02, 6.61 ± 4.18, 6.82 ± 4.26, and 6.91 ± 4.43; Fig. 5D). Interestingly, for ON-OFF and ETC types, $D_{vR,AVG}$ values of *wt* RGCs were larger than those of any age group of *rd10* mice and significantly higher than those of ON or OFF RGCs in *wt* mice. This indicates that the spiking responses of ON-OFF and ETC cells are intrinsically more variable compared to ON and OFF cells.

As mentioned in **Materials and Methods** section, D_{vR} calculation method emphasizes capturing precise temporal variations rather than assessing overall correlation. (Nirenberg and Latham, 2003; Satuvuori and Kreuz, 2018). This focus on precise temporal variations may account for the discrepancies observed between STTC and D_{vR}. In other words, the systematic increase in $STTC_{AVG}$ and the fluctuating trends in $D_{vR,AVG}$ may reflect each metric's nature of differing sensitivities to temporal precision. For example, in *rd10* OFF cells, both STTC and D_{vR} decreased when comparing early (P15) and advanced (P60) stages of degeneration. However, between P20 and P30, while STTC showed no statistically significant inter-trial inconsistency, $D_{vR,AVG}$ showed a notable shift, with a ~31.6% increase in spike timing variability. This change was substantially larger than the difference observed between P15 and P20 (~6.5%) and even reversed the trend, highlighting that subtle discrepancies in spike timing variability can be detected by D_{vR} even when STTC shows no apparent differences.

3.3. Retinal degeneration increases spike count variability

Lastly, Fano factors (FFs) were calculated to assess the variability in the number of spikes elicited across trials. Our FF analysis revealed a tendency for an abrupt increase in average FF values (FF_{AVG}) at the advanced stage of retinal degeneration (P60) in both ON (0.74 ± 1.27, 0.66 ± 1.22, 0.67 ± 1.4, 0.63 ± 1.13, and 1.17 ± 2.08 for *wt*, *rd10* P15, P20, P30, and P60; Fig. 6Ai) and OFF cells (0.64 ± 1.08, 0.54 ± 1.06, 0.45 ± 0.89, 0.46 ± 0.87, and 0.8 ± 1.62; Fig. 6Aii). In sharp contrast, ON-OFF and ETC cells exhibited downward trend in FF_{AVG} values as retinal degeneration progressed: FF_{AVG} values of ON-OFF cells were 0.77 ± 1.38, 1.14 ± 2.06, 1.03 ± 1.47, 0.59 ± 1.1, and 0.66 ± 1.18 (Fig. 6Aiii), while the FF_{AVG} values of ETC cells were 0.69 ± 1.32, 0.91 ± 2, 0.83 ± 1.91, 0.76 ± 2.22, and 0.77 ± 1.81 (Fig. 6Aiv). Intriguingly, the FFs of all RGC types in *wt* mice were relatively similar (0.74 ± 1.27, 0.64 ± 1.08, 0.77 ± 1.38, 0.69 ± 1.32 for ON, OFF, ON-OFF, and ETC cells, respectively), indicating that spike count variability was minimal across RGC types in the healthy retinas. For *rd10* mice, it is worth to note that ON and OFF cells showed a sudden increase in FF_{AVG} value at P60

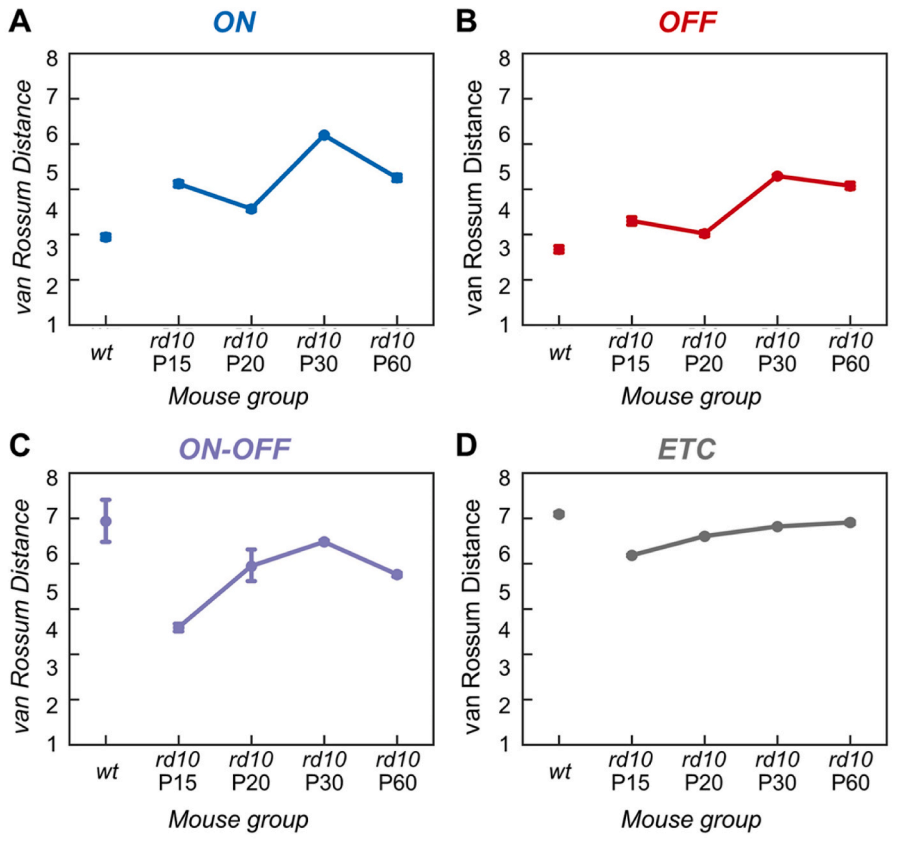

Fig. 5. Van Rossum distance (D_{vR}) unveils decremental tendency of inter-trial spike timing consistency in perspective of precise spike timings. $D_{vR,AVG}$ values of (**A**) ON, (**B**) OFF, (**C**) ON-OFF and (**D**) ETC cells. Error bars indicate the confidence interval of the $D_{vR,AVG}$. Tight confidence intervals resulted in error bars almost indistinguishable from the data point.

(right-most bars in Fig. 6Ai and 6Aii) after remaining relatively constant throughout younger ages ranging from P15 to P30. Conversely, ON-OFF and ETC cells exhibited larger FF_{AVG} values in the earlier stages of degeneration (P15 and P20) compared to the later stages (P30 and P60) (*see* **Discussion**).

FF are typically inversely correlated with the firing rate of healthy neuron (Barlow and Levick, 1969; Kara et al., 2000). To avoid potential misinterpretation arising from the observed decline in firing rates during retinal degeneration, we analyzed FF values in relation to firing rate along with Pearson's correlation coefficient (*r* value) (Fig. 6B). Interestingly, ON, ON-OFF, and ETC cells displayed positive Pearson's *r* value at every stage of retinal degeneration in *rd10* mice (Fig. 6Bi-6Biv). The OFF cells of *rd10* P15 and P20 were the only conditions where negative Pearson's *r* values were observed, but these correlations were very weak due to their small magnitude ($|r| < 0.1$). Taken all together, our results suggest that the increase in FF values cannot be attributed solely to the decrease in firing rate. This indicates the involvement of additional factors. We hypothesize that the primary contributor to the observed increase in FF is the progression of retinal degeneration itself (*see* **Discussion**).

4. Discussion

4.1. Impact of retinal degeneration on neural coding stability differs in RGC types

In this study, the spiking activities of RGCs in *rd10* mice showed substantially reduced consistencies across repeated presentations of the same visual stimulus compared to those of *wt* mice in the both aspects we examined (*i.e.*, timing and count), even during the intermediate stages of retinal degeneration (*e.g.*, P30). It is well known that the precise timing is essential for the reproducibility of visual processing (Buračas and Albright, 1999; VanRullen et al., 2005; Warzecha and Egelhaaf, 1999; Zador, 1998). Thus, the consistencies of spike timing and count across trials are crucial components of healthy RGC signaling (Berry et al., 1997; Kara et al., 2000; Koch et al., 2004; Meister and Berry, 1999; Puchalla et al., 2005; Reich et al., 1997; Uzzell and Chichilnisky, 2004).

We found distinct trends across different RGC types in the inter-trial firing consistency deterioration resulted from the degeneration. In particular, examining the relative changes of *rd10* STTC values in comparison with *wt* STTC values revealed that degeneration impacts the ON and OFF pathways asymmetrically: degeneration resulted in sharper declines in the $STTC_{AVG}$ of ON cells up to ~84.7% between *wt* and *rd10* P60 groups (Fig. 4Bi) compared to the more gradual decline of ~63.0% in the $STTC_{AVG}$ of OFF cells in the $STTC_{AVG}$ of OFF cells between the same groups (Fig. 4Bii).

The asymmetry between the ON and OFF pathways has been widely reported in prior studies (Chichilnisky and Kalmar, 2002; Jin et al., 2011; Komban et al., 2014; Kremkow et al., 2014; Nichols et al., 2013; Zaghloul et al., 2003; Im and Fried, 2015, 2016; Im et al., 2018). This asymmetry may stem from differences in the intrinsic properties of each pathway, such as ion channel density and distribution (Goldman et al., 2001; Guo et al., 2016). Higher densities of specific ion channels in ON cells might confer greater resilience to degeneration, allowing them to maintain more stable signaling patterns even as degeneration progresses. Conversely, the OFF pathway may lack these stabilizing properties, making it more vulnerable to the disruptive effects of degeneration. Moreover, this difference between the two pathways may be due to an imbalance in the rate of rod and cone degeneration. In *rd10* mice, rod degeneration reaches its peak between P21 and P25 (Biswas

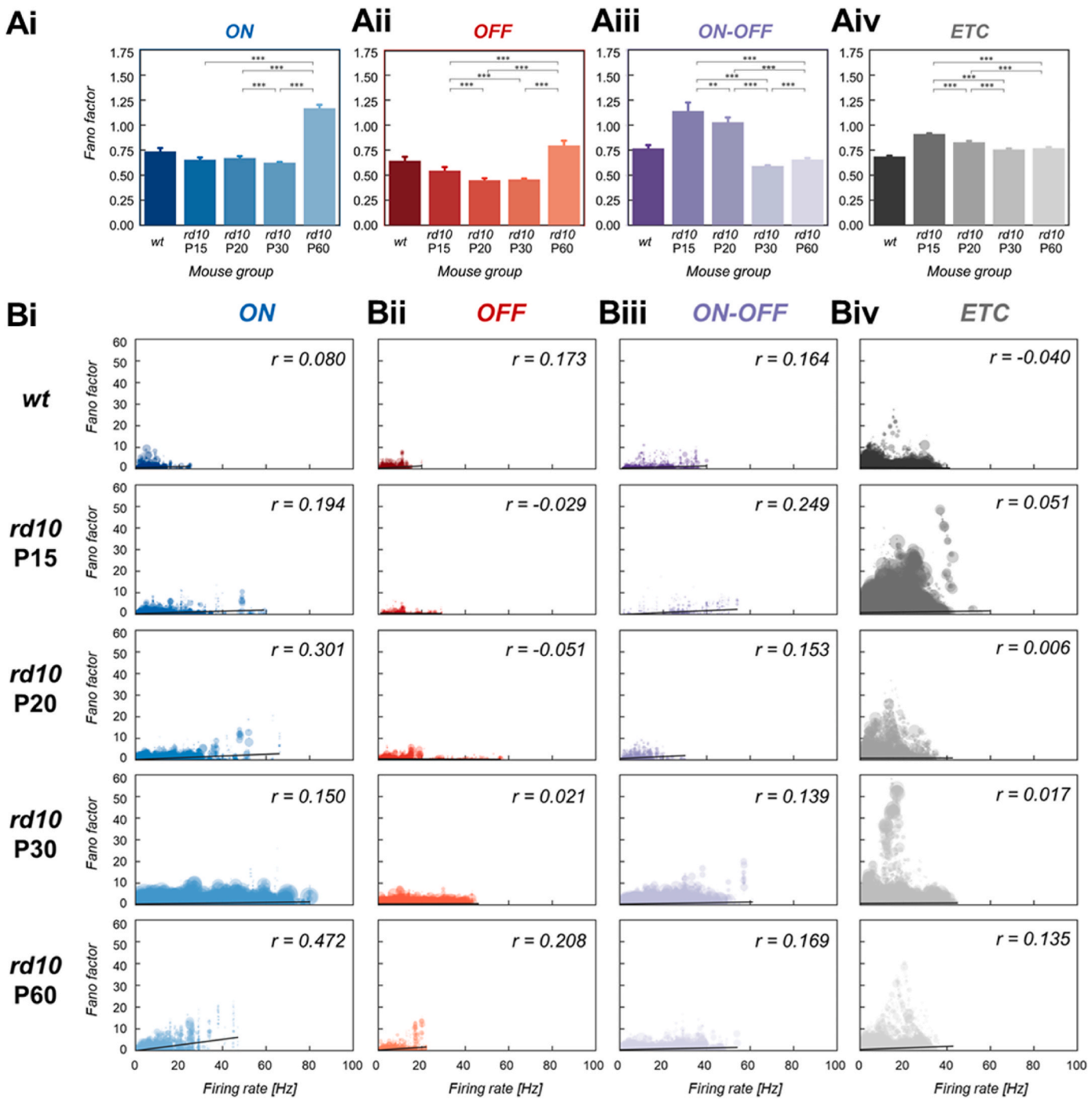

Fig. 6. Increase in inter-spike inconsistency in perspective of Fano factor (FF). **(A)** The FF_{AVG} for the delayed responses of ON (Ai), OFF (Aii), ON-OFF (Aiii), and ETC cells (Aiv) were calculated for each mouse group. Error bars indicate the confidence interval of the FF_{AVG}. **(B)** FFs plotted as a function of firing rate. Size of a circle indicates the number of trials fall in that range. A solid line is a linear regression of the data, and Pearson's *r* value is annotated in the corner of each panel.

et al., 2014), while cone deterioration starts around P60, with only a few surviving by P180 (Phillips et al., 2010). The loss of rods enhances synaptic conductance in depolarizing rod bipolar cells, whereas cone degeneration decreases conductance in OFF bipolar cells and elevates it in ON bipolar cells. These synaptic modifications impact narrow-field, bistratified amacrine cells, ultimately leading to distinct ON and OFF responses to photoreceptor loss (Ly et al., 2022).

Examination of STTC trends from a broader perspective revealed a more distinct grouping when contrast-sensing neurons (ON, OFF, and ON-OFF cells) were compared with ETC cells. While contrast-sensing neurons exhibited minor individual differences, they collectively exhibited consistent changing patterns with aligned STTC trends across these cell types (Fig. 4Bi-4Biii). In contrast, ETC cells showed no clear trend with respect to the progression of retinal degeneration (Fig. 4Biv). The ambiguous results in the STTC values of ETC cells might be due to inaccurate classification, potentially including various RGC types. This could obscure the unique characteristics of each cell type. By refining classifications to tease more specific RGC types out, such as directionally selective (DS) cells (Barlow and Hill, 1963; Fried et al., 2002; Trenholm et al., 2011), we may achieve a clearer and deeper insights how distinct retinal circuitries are differentially affected by outer retinal degeneration.

Spike count variability displayed a distinct trend from spike timing variability as retinal degeneration progressed. For example, while the spike timing variabilities systematically increased in all RGC types except ETC cells (Fig. 4), the spike count variabilities stayed relatively stable in ON RGCs (Fig. 6Ai) or showed slight to significant decreases in OFF and ON-OFF RGCs (Fig. 6Aii and 6Aiii) during the early to intermediate stages of degeneration (P15-P30). Interestingly, both *rd10* ON and OFF cells exhibited a sudden increase in FF_{AVG} at P60. This abrupt increase in spike count variability was shown not to result from reduced firing rates as plotting FF values against firing rate (Fig. 6Bi-6Biii) rejected the established inverse correlation between spike count variability and firing rate (Barlow and Levick, 1969; Kara et al., 2000). Instead, the increase in FF_{AVG} is likely attributable to elevated spontaneous activities caused by the progression of degeneration (Stasheff, 2008; Margolis et al., 2008; Sekirnjak et al., 2011; Stasheff et al., 2011; Cho et al., 2016). However, it remains unclear why the FF values of ON-OFF RGCs did not increase at P60 (Fig. 6Aiii), possibly suggesting that retinal degeneration affects the ON-OFF pathway differently from the ON or OFF pathways.

4.2. Possible mechanisms of increased inter-trial variability of spike timing and spike count

The increased inter-trial variability in the spiking activity of RGCs in response to repetitive light stimuli observed in this study may stem from several potential mechanisms, each contributing to the instability of visual signal processing in degenerative retinas. Possible contributors include photoreceptor degeneration, extensive rewiring of the retinal network, inflammation and glial cell activation, and disruptions in presynaptic neurons.

First, the degeneration of photoreceptors and subsequent rewiring of the retinal network are key factors contributing to the increased variability in RGC responses. These changes disrupt the stable input to downstream neurons like bipolar cells and RGCs. As photoreceptors degenerate, surviving neurons like bipolar and amacrine cells form *de novo* connections in response to the loss of photoreceptor input (Euler and Schubert, 2015; Marc et al., 2003). While this rewiring might reflect neurons' attempts to seek synaptic excitation (Jones et al., 2003), the new circuitry is likely to disrupt visual processing (Strettoi et al., 2003). This may result in irregular responses to visual stimuli and increased variability in both spike timing and count across trials (Fariss et al., 2000). Additionally, spontaneous RGC activity rises as photoreceptors degenerate, driven by abnormal spiking from inner retinal cells such as amacrine cells, further increasing variability in stimulus-driven responses (Stasheff, 2008). The loss of precise light-evoked responses found in our study suggests a possibility that this growing instability in the retina could affect visual signal processing in the higher visual centers as degeneration progresses (Kara et al., 2000).

Second, inflammation and activation of glial cells, including Müller glia and microglia, may also contribute to the increased instability by altering the retinal microenvironment, affecting neuron excitability and spike timing variability (Bringmann et al., 2006). Müller cells, which envelop synapses in the retina, can directly stimulate post-synaptic neurons by releasing and re-uptaking neurotransmitters, producing excitatory or inhibitory responses (Vecino et al., 2016). Dysfunction or degeneration of these glial cells can lead to inconsistent firing pattern of RGCs, further destabilizing visual signal processing.

Lastly, disruptions in synaptic transmission from bipolar cells and imbalances in excitatory-inhibitory (E/I) control from amacrine cells may contribute to greater variability in RGC responses (Margolis et al., 2008). These changes compromise the precise modulation of retinal outputs, exacerbating the variability found in the present study. Any combination of these potential mechanisms could underlie the variability in neural responses observed during retinal degeneration.

One limitation of this study is that our analysis focused solely on recording and assessing the responses of RGCs, without addressing the roles of other criticial components of the retinal circuitry. A comprehensive investigation of the entire retinal network, including presynaptic neurons like bipolar cells and interneurons such as amacrine and horizontal cells, is essential to fully understand the mechanisms underlying increased variabilities of RGC responses. These presynaptic neurons and interneurons are integral to modulating retinal signal processing, and their interactions with RGCs likely influence the overall effects of degeneration on retinal function. Future studies should adopt a broader approach that incorporates the entire retinal network, providing deeper insights into how degeneration affects retinal circuitry as a whole. Such an approach is critical for advancing our understanding of the disease progression and developing more effective therapeutic strategies.

4.3. Clinical implication of this work

Our findings offer valuable insights into the disruptions in neural coding that occur during retinal degeneration, as observed in conditions such as RP and AMD. (Alexander et al., 1995; Arimura et al., 2011; Tejeria, 2002; Wittich et al., 2011). For instance, Alexander et al. reported inconsistent visual perception in patients at advanced stage of RP in their study that examined a quantitative relationship between foveal visual acuity and contrast sensitivity (Alexander et al., 1995). Meanwhile, Arimura et al. also reported a descriptive narrative for the distorted and incongruent perception of AMD patients (Arimura et al., 2011).

A deeper understanding of the decline in spiking pattern consistency can contribute to the advancements in visual prostheses for individuals with retinal degenerative diseases. Once commercially available but now discontinued prosthetic devices, such as Argus® II Retinal Prosthesis System by Second Sight II (Castaldi et al., 2016; da Cruz et al., 2013; Kotecha et al., 2014) and Alpha-IMS/AMS by Retina Implant AG (Edwards et al., 2018; Stingl et al., 2013; Zrenner et al., 2012), were built for RP patients. Additionally, clinical trial-stage devices like PRIMA by Pixium Vision (now by Science Corp.) for AMD patients (Palanker et al., 2020; Wang et al., 2022) are about to be commercialized. All of these devices aim to restore vision by electrically stimulating the remaining retinal neurons to evoke artificial visual perceptions. Despite technological advances, their performance remains far below the level of natural vision. Understanding how retinal degeneration alters spiking patterns is essential for designing effective retinal prostheses that can compensate for these changes. In addition to our previous study reporting the increased spiking inconsistencies in electrically-evoked responses of degenerate retinas (Yoon et al., 2020), our finding of the present study further supports that RGC spiking responses become substantially inconsistent, suggesting decreased stability of the retinal network and/or RGCs themselves. Therefore, the development of appropriate stimulating method(s) which produce consistent RGC spiking responses is necessary for the improved quality and reliability of prosthetic vision for individuals with severe retinal degeneration.

5. Conclusions

This study addresses an unexplored gap in understanding how retinal degeneration afffects the spiking activity of RGCs in response to light stimuli. By examining spike timing and count variabilities across repeated presentations of the same visual stimulus in *rd10* mouse retinas at different stages of RP, we found that RGCs in *rd10* mice exhibited decreasing spiking consistencies across trials as retinal degeneration progressed, compared to those of RGCs in *wt* mice. Moreover, the changes in inter-trial variability differed across RGC types, indicating that retinal degeneration affects different cell types in distinct ways. These findings highlight the importance of incorporating healthy neural coding features, such as reliable spike frequency and precise temporal precision, into retinal prosthetics and optogenetic interventions for visual rehabilitation. Preserving these features could significantly improve

the quality and reliability of vision restoration, emphasizing the need for sophisticated cell-type-specific stimulation strategies.

CRediT authorship contribution statement

Da Eun Kim: Writing – original draft, Visualization, Software, Methodology, Investigation, Formal analysis, Data curation. **Sein Kim:** Writing – original draft, Visualization, Software, Methodology, Investigation, Formal analysis, Data curation. **Minju Kim:** Software, Methodology, Formal analysis, Data curation. **Byoung-Kyong Min:** Writing – review & editing, Supervision. **Maesoon Im:** Writing – review & editing, Supervision, Funding acquisition, Conceptualization.

Data availability

The data that support the findings of this study are available upon reasonable request from the authors.

Funding

This work was supported in part by KIST (Korea Institute of Science and Technology) institutional grants (2E33881 and 2E33682), and in part by the National R&D Program through the National Research Foundation (NRF) of Korea funded by the Ministry of Science and ICT (2020R1C1C1006065 and 2022M3E5E8017395).

Declaration of competing interest

None.

Acknowledgements

None.

Abbreviations

RGC	retinal ganglion cell
wt	wild type
STTC	spike time-tilling coefficient
FF	Fano factor
D_{vR}	van Rossum distance

Data availability

Data will be made available on request.

References

Alexander, K.R., Derlacki, D.J., Fishman, G.A., 1995. Visual acuity vs letter contrast sensitivity in retinitis pigmentosa. Vis. Res. 35, 1495–1499. https://doi.org/10.1016/0042-6989(95)98729-S.

Arimura, E., Matsumoto, C., Nomoto, H., Hashimoto, S., Takada, S., Okuyama, S., Shimomura, Y., 2011. Correlations between M-CHARTS and PHP findings and subjective perception of metamorphopsia in patients with macular diseases. Investig. Ophthalmol. Vis. Sci. 52, 128. https://doi.org/10.1167/iovs.09-3535.

Baden, T., Berens, P., Franke, K., Román Rosón, M., Bethge, M., Euler, T., 2016. The functional diversity of retinal ganglion cells in the mouse. Nature 529, 345–350. https://doi.org/10.1038/nature16468.

Barhoum, R., Martínez-Navarrete, G., Corrochano, S., Germain, F., Fernandez-Sanchez, L., de la Rosa, E.J., de la Villa, P., Cuenca, N., 2008. Functional and structural modifications during retinal degeneration in the rd10 mouse. Neuroscience 155, 698–713. https://doi.org/10.1016/j.neuroscience.2008.06.042.

Barlow, H.B., Hill, R.M., 1963. Selective sensitivity to direction of movement in ganglion cells of the rabbit retina. Science 139, 412–414. https://doi.org/10.1126/science.139.3553.412.

Barlow, H.B., Levick, W.R., 1969. Changes in the maintained discharge with adaptation level in the cat retina. J. Physiol. 202, 699–718. https://doi.org/10.1113/jphysiol.1969.sp008836.

Berry, M.J., Warland, D.K., Meister, M., 1997. The structure and precision of retinal spike trains. Proc. Natl. Acad. Sci. USA 94, 5411–5416. https://doi.org/10.1073/pnas.94.10.5411.

Biswas, S., Haselier, C., Mataruga, A., Thumann, G., Walter, P., Müller, F., 2014. Pharmacological analysis of intrinsic neuronal oscillations in rd10 retina. PLoS One 9, e99075. https://doi.org/10.1371/journal.pone.0099075.

Bringmann, A., Pannicke, T., Grosche, J., Francke, M., Wiedemann, P., Skatchkov, S., Osborne, N., Reichenbach, A., 2006. Müller cells in the healthy and diseased retina. Prog. Retin. Eye Res. 25, 397–424. https://doi.org/10.1016/j.preteyeres.2006.05.003.

Buccino, A.P., Hurwitz, C.L., Garcia, S., Magland, J., Siegle, J.H., Hurwitz, R., Hennig, M. H., 2020. SpikeInterface, a unified framework for spike sorting. Elife 9. https://doi.org/10.7554/eLife.61834.

Buračas, G.T., Albright, T.D., 1999. Gauging sensory representations in the brain. Trends Neurosci. 22, 303–309. https://doi.org/10.1016/S0166-2236(98)01376-9.

Carcieri, S.M., Jacobs, A.L., Nirenberg, S., 2003. Classification of retinal ganglion cells: a statistical approach. J. Neurophysiol. 90, 1704–1713. https://doi.org/10.1152/jn.00127.2003.

Castaldi, E., Cicchini, G.M., Cinelli, L., Biagi, L., Rizzo, S., Morrone, M.C., 2016. Visual BOLD response in late blind subjects with Argus II retinal prosthesis. PLoS Biol. 14, e1002569. https://doi.org/10.1371/journal.pbio.1002569.

Cha, S., Ahn, J., Jeong, Y., Lee, Y.H., Kim, H.K., Lee, D., Yoo, Y., Goo, Y.S., 2022. Stage-dependent changes of visual function and electrical response of the retina in the rd10 mouse model. Front. Cell. Neurosci. 16. https://doi.org/10.3389/fncel.2022.926096.

Chichilnisky, E.J., Kalmar, R.S., 2002. Functional asymmetries in ON and OFF ganglion cells of primate retina. J. Neurosci. 22, 2737–2747. https://doi.org/10.1523/JNEUROSCI.22-07-02737.2002.

Cho, A., Ratliff, C., Sampath, A., Weiland, J., 2016. Changes in ganglion cell physiology during retinal degeneration influence excitability by prosthetic electrodes. J. Neural. Eng. 13, 025001. https://doi.org/10.1088/1741-2560/13/2/025001.

Cowan, C.S., Renner, M., De Gennaro, M., Gross-Scherf, B., Goldblum, D., Hou, Y., Munz, M., Rodrigues, T.M., Krol, J., Szikra, T., Cuttat, R., Waldt, A., Papasaikas, P., Diggelmann, R., Patino-Alvarez, C.P., Galliker, P., Spirig, S.E., Pavlinic, D., Gerber-Hollbach, N., Schuierer, S., Srdanovic, A., Balogh, M., Panero, R., Kusnyerik, A., Szabo, A., Stadler, M.B., Orgül, S., Picelli, S., Hasler, P.W., Hierlemann, A., Scholl, H. P.N., Roma, G., Nigsch, F., Roska, B., 2020. Cell types of the human retina and its organoids at single-cell resolution. Cell 182, 1623–1640.e34. https://doi.org/10.1016/j.cell.2020.08.013.

Cutts, C.S., Eglen, S.J., 2014. Detecting pairwise correlations in spike trains: an objective comparison of methods and application to the study of retinal waves. J. Neurosci. 34, 14288–14303. https://doi.org/10.1523/JNEUROSCI.2767-14.2014.

da Cruz, L., Coley, B.F., Dorn, J., Merlini, F., Filley, E., Christopher, P., Chen, F.K., Wuyyuru, V., Sahel, J., Stanga, P., Humayun, M., Greenberg, R.J., Dagnelie, G., 2013. The Argus II epiretinal prosthesis system allows letter and word reading and long-term function in patients with profound vision loss. Br. J. Ophthalmol. 97, 632–636. https://doi.org/10.1136/bjophthalmol-2012-301525.

Edwards, T.L., Cottriall, C.L., Xue, K., Simunovic, M.P., Ramsden, J.D., Zrenner, E., MacLaren, R.E., 2018. Assessment of the electronic retinal implant Alpha AMS in restoring vision to blind patients with end-stage retinitis pigmentosa. Ophthalmology 125, 432–443. https://doi.org/10.1016/j.ophtha.2017.09.019.

Euler, T., Schubert, T., 2015. Multiple independent oscillatory networks in the degenerating retina. Front. Cell. Neurosci. 9. https://doi.org/10.3389/fncel.2015.00444.

Fariss, R.N., Li, Z.-Y., Milam, A.H., 2000. Abnormalities in rod photoreceptors, amacrine cells, and horizontal cells in human retinas with retinitis pigmentosa. Am. J. Ophthalmol. 129, 215–223. https://doi.org/10.1016/S0002-9394(99)00401-8.

Fried, S.I., Münch, T.A., Werblin, F.S., 2002. Mechanisms and circuitry underlying directional selectivity in the retina. Nature 420, 411–414. https://doi.org/10.1038/nature01179.

Gabbiani, F., Cox, S.J., 2017. Quantification of spike train variability. In: Mathematics for Neuroscientists. Elsevier, pp. 321–334. https://doi.org/10.1016/B978-0-12-801895-8.00017-8.

Gargini, C., Terzibasi, E., Mazzoni, F., Strettoi, E., 2007. Retinal organization in the retinal degeneration 10 (rd10) mutant mouse: a morphological and ERG study. J. Comp. Neurol. 500, 222–238. https://doi.org/10.1002/cne.21144.

Goldman, M.S., Golowasch, J., Marder, E., Abbott, L.F., 2001. Global structure, robustness, and modulation of neuronal models. J. Neurosci. 21, 5229–5238. https://doi.org/10.1523/JNEUROSCI.21-14-05229.2001.

Guo, T., Tsai, D., Morley, J.W., Suaning, G.J., Kameneva, T., Lovell, N.H., Dokos, S., 2016. Electrical activity of ON and OFF retinal ganglion cells: a modelling study. J. Neural. Eng. 13, 025005. https://doi.org/10.1088/1741-2560/13/2/025005.

Guymer, R.H., Campbell, T.G., 2023. Age-related macular degeneration. Lancet 401, 1459–1472. https://doi.org/10.1016/S0140-6736(22)02609-5.

Hartong, D.T., Berson, E.L., Dryja, T.P., 2006. Retinitis pigmentosa. Lancet 368, 1795–1809. https://doi.org/10.1016/S0140-6736(06)69740-7.

Im, M., Fried, S.I., 2015. Indirect activation elicits strong correlations between light and electrical responses in ON but not OFF retinal ganglion cells. J. Physiol. 593, 3577–3596. https://doi.org/10.1113/JP270606.

Im, M., Fried, S.I., 2016. Temporal properties of network-mediated responses to repetitive stimuli are dependent upon retinal ganglion cell type. J. Neural. Eng. 13, 025002. https://doi.org/10.1088/1741-2560/13/2/025002.

Im, M., Werginz, P., Fried, S.I., 2018. Electric stimulus duration alters network-mediated responses depending on retinal ganglion cell type. J. Neural. Eng. 15, 036010. https://doi.org/10.1088/1741-2552/aaadc1.

Jin, J., Wang, Y., Lashgari, R., Swadlow, H.A., Alonso, J.-M., 2011. Faster thalamocortical processing for dark than light visual targets. J. Neurosci. 31, 17471–17479. https://doi.org/10.1523/JNEUROSCI.2456-11.2011.

Jones, B.W., Pfeiffer, R.L., Ferrell, W.D., Watt, C.B., Marmor, M., Marc, R.E., 2016a. Retinal remodeling in human retinitis pigmentosa. Exp. Eye Res. 150, 149–165. https://doi.org/10.1016/j.exer.2016.03.018.

Jones, Bryan W., Pfeiffer, R.L., Ferrell, W.D., Watt, C.B., Tucker, J., Marc, R.E., 2016b. Retinal remodeling and metabolic alterations in human AMD. Front. Cell. Neurosci. 10. https://doi.org/10.3389/fncel.2016.00103.

Jones, B.W., Watt, C.B., Frederick, J.M., Baehr, W., Chen, C., Levine, E.M., Milam, A.H., Lavail, M.M., Marc, R.E., 2003. Retinal remodeling triggered by photoreceptor degenerations. J. Comp. Neurol. 464, 1–16. https://doi.org/10.1002/cne.10703.

Kara, P., Reinagel, P., Reid, R.C., 2000. Low response variability in simultaneously recorded retinal, thalamic, and cortical neurons. Neuron 27, 635–646. https://doi.org/10.1016/S0896-6273(00)00072-6.

Koch, K., McLean, J., Berry, M., Sterling, P., Balasubramanian, V., Freed, M.A., 2004. Efficiency of information transmission by retinal ganglion cells. Curr. Biol. 14, 1523–1530. https://doi.org/10.1016/j.cub.2004.08.060.

Komban, S.J., Kremkow, J., Jin, J., Wang, Y., Lashgari, R., Li, X., Zaidi, Q., Alonso, J.-M., 2014. Neuronal and perceptual differences in the temporal processing of darks and lights. Neuron 82, 224–234. https://doi.org/10.1016/j.neuron.2014.02.020.

Kotecha, A., Zhong, J., Stewart, D., da Cruz, L., 2014. The Argus II prosthesis facilitates reaching and grasping tasks: a case series. BMC Ophthalmol. 14, 71. https://doi.org/10.1186/1471-2415-14-71.

Kremkow, J., Jin, J., Komban, S.J., Wang, Y., Lashgari, R., Li, X., Jansen, M., Zaidi, Q., Alonso, J.-M., 2014. Neuronal nonlinearity explains greater visual spatial resolution for darks than lights. Proc. Natl. Acad. Sci. U. S. A. 111, 3170–3175. https://doi.org/10.1073/pnas.1310442111.

Livingstone, M., Hubel, D., 1987. Psychophysical evidence for separate channels for the perception of form, color, movement, and depth. J. Neurosci. 7, 3416–3468. https://doi.org/10.1523/JNEUROSCI.07-11-03416.1987.

Ly, K., Guo, T., Tsai, D., Muralidharan, M., Shivdasani, M.N., Lovell, N.H., Dokos, S., 2022. Simulating the impact of photoreceptor loss and inner retinal network changes on electrical activity of the retina. J. Neural. Eng. 19, 065002. https://doi.org/10.1088/1741-2552/aca221.

Marc, R.E., Jones, B.W., 2003. Retinal remodeling in inherited photoreceptor degenerations. Mol. Neurobiol. 28, 139–148. https://doi.org/10.1385/MN:28:2:139.

Marc, R.E., Jones, B.W., Watt, C.B., Strettoi, E., 2003. Neural remodeling in retinal degeneration. Prog. Retin. Eye Res. 22, 607–655. https://doi.org/10.1016/S1350-9462(03)00039-9.

Margolis, D.J., Newkirk, G., Euler, T., Detwiler, P.B., 2008. Functional stability of retinal ganglion cells after degeneration-induced changes in synaptic Input. J. Neurosci. 28, 6526–6536. https://doi.org/10.1523/JNEUROSCI.1533-08.2008.

Meister, M., Berry, M.J., 1999. The neural code of the retina. Neuron 22, 435–450. https://doi.org/10.1016/S0896-6273(00)80700-X.

Nichols, Z., Nirenberg, S., Victor, J., 2013. Interacting linear and nonlinear characteristics produce population coding asymmetries between ON and OFF cells in the retina. J. Neurosci. 33, 14958–14973. https://doi.org/10.1523/JNEUROSCI.1004-13.2013.

Nirenberg, S., Latham, P.E., 2003. Decoding neuronal spike trains: how important are correlations? Proc. Natl. Acad. Sci. USA 100, 7348–7353. https://doi.org/10.1073/pnas.1131895100.

Palanker, D., Le Mer, Y., Mohand-Said, S., Muqit, M., Sahel, J.A., 2020. Photovoltaic restoration of central vision in atrophic age-related macular degeneration. Ophthalmology 127, 1097–1104. https://doi.org/10.1016/j.ophtha.2020.02.024.

Phillips, M.J., Otteson, D.C., Sherry, D.M., 2010. Progression of neuronal and synaptic remodeling in the rd10 mouse model of retinitis pigmentosa. J. Comp. Neurol. 518, 2071–2089. https://doi.org/10.1002/cne.22322.

Piano, I., Novelli, E., Gasco, P., Ghidoni, R., Strettoi, E., Gargini, C., 2013. Cone survival and preservation of visual acuity in an animal model of retinal degeneration. Eur. J. Neurosci. 37, 1853–1862. https://doi.org/10.1111/ejn.12196.

Puchalla, J.L., Schneidman, E., Harris, R.A., Berry, M.J., 2005. Redundancy in the population code of the retina. Neuron 46, 493–504. https://doi.org/10.1016/j.neuron.2005.03.026.

Reich, D.S., Victor, J.D., Knight, B.W., Ozaki, T., Kaplan, E., 1997. Response variability and timing precision of neuronal spike trains in vivo. J. Neurophysiol. 77, 2836–2841. https://doi.org/10.1152/jn.1997.77.5.2836.

Remington, L.A., 2012. Visual pathway. In: Clinical Anatomy and Physiology of the Visual System. Elsevier, pp. 233–252. https://doi.org/10.1016/B978-1-4377-1926-0.10013-X.

Roska, B., Werblin, F., 2001. Vertical interactions across ten parallel, stacked representations in the mammalian retina. Nature 410, 583–587. https://doi.org/10.1038/35069068.

Satuvuori, E., Kreuz, T., 2018. Which spike train distance is most suitable for distinguishing rate and temporal coding? J. Neurosci. Methods 299, 22–33. https://doi.org/10.1016/j.jneumeth.2018.02.009.

Schiller, P.H., 1995. The ON and OFF channels of the mammalian visual system. Prog. Retin. Eye Res. 15, 173–195. https://doi.org/10.1016/1350-9462(95)00009-7.

Schiller, P.H., Sandell, J.H., Maunsell, J.H.R., 1986. Functions of the ON and OFF channels of the visual system. Nature 322, 824–825. https://doi.org/10.1038/322824a0.

Sekirnjak, C., Jepson, L.H., Hottowy, P., Sher, A., Dabrowski, W., Litke, A.M., Chichilnisky, E.J., 2011. Changes in physiological properties of rat ganglion cells during retinal degeneration. J. Neurophysiol. 105, 2560–2571. https://doi.org/10.1152/jn.01061.2010.

Stasheff, S.F., 2008. Emergence of sustained spontaneous hyperactivity and temporary preservation of OFF responses in ganglion cells of the retinal degeneration (rd1) mouse. J. Neurophysiol. 99, 1408–1421. https://doi.org/10.1152/jn.00144.2007.

Stasheff, S.F., Shankar, M., Andrews, M.P., 2011. Developmental time course distinguishes changes in spontaneous and light-evoked retinal ganglion cell activity in rd1 and rd10 mice. J. Neurophysiol. 105, 3002–3009. https://doi.org/10.1152/jn.00704.2010.

Stingl, K., Bartz-Schmidt, K.U., Besch, D., Braun, A., Bruckmann, A., Gekeler, F., Greppmaier, U., Hipp, S., Hörtdörfer, G., Kernstock, C., Koitschev, A., Kusnyerik, A., Sachs, H., Schatz, A., Stingl, K.T., Peters, T., Wilhelm, B., Zrenner, E., 2013. Artificial vision with wirelessly powered subretinal electronic implant alpha-IMS. Process Biochem. (Oxford, U. K.): Biol. Sci. 280, 20130077. https://doi.org/10.1098/rspb.2013.0077.

Strettoi, E., Pignatelli, V., Rossi, C., Porciatti, V., Falsini, B., 2003. Remodeling of second-order neurons in the retina of rd/rd mutant mice. Vis. Res. 43, 867–877. https://doi.org/10.1016/S0042-6989(02)00594-1.

Tejeria, L., 2002. Face recognition in age related macular degeneration: perceived disability, measured disability, and performance with a bioptic device. Br. J. Ophthalmol. 86, 1019–1026. https://doi.org/10.1136/bjo.86.9.1019.

Trenholm, S., Johnson, K., Li, X., Smith, R.G., Awatramani, G.B., 2011. Parallel mechanisms encode direction in the retina. Neuron 71, 683–694. https://doi.org/10.1016/j.neuron.2011.06.020.

Uzzell, V.J., Chichilnisky, E.J., 2004. Precision of spike trains in primate retinal ganglion cells. J. Neurophysiol. 92, 780–789. https://doi.org/10.1152/jn.01171.2003.

Van Rossum, M.C.W., 2001. A novel spike distance. Neural Comput. 13, 751–763. https://doi.org/10.1162/089976601300014321.

VanRullen, R., Guyonneau, R., Thorpe, S.J., 2005. Spike times make sense. Trends Neurosci. 28, 1–4. https://doi.org/10.1016/j.tins.2004.10.010.

Vecino, E., Rodriguez, F.D., Ruzafa, N., Pereiro, X., Sharma, S.C., 2016. Glia–neuron interactions in the mammalian retina. Prog. Retin. Eye Res. 51, 1–40. https://doi.org/10.1016/j.preteyeres.2015.06.003.

Wang, B.-Y., Chen, Z.C., Bhuckory, M., Huang, T., Shin, A., Zuckerman, V., Ho, E., Rosenfeld, E., Galambos, L., Kamins, T., Mathieson, K., Palanker, D., 2022. Electronic photoreceptors enable prosthetic visual acuity matching the natural resolution in rats. Nat. Commun. 13, 6627. https://doi.org/10.1038/s41467-022-34353-y.

Warzecha, A.-K., Egelhaaf, M., 1999. Variability in spike trains during constant and dynamic stimulation. Science 283, 1927–1930. https://doi.org/10.1126/science.283.5409.1927.

Wässle, H., 2004. Parallel processing in the mammalian retina. Nat. Rev. Neurosci. 5, 747–757. https://doi.org/10.1038/nrn1497.

Wittich, W., Watanabe, D.H., Kapusta, M.A., Overbury, O., 2011. Subjective perception of visual distortions or scotomas in individuals with retinitis pigmentosa. J. Vis. Impair. Blind. (JVIB) 105, 50–55. https://doi.org/10.1177/0145482X1110500106.

Yger, P., Spampinato, G.L., Esposito, E., Lefebvre, B., Deny, S., Gardella, C., Stimberg, M., Jetter, F., Zeck, G., Picaud, S., Duebel, J., Marre, O., 2018. A spike sorting toolbox for up to thousands of electrodes validated with ground truth recordings in vitro and in vivo. Elife 7. https://doi.org/10.7554/eLife.34518.

Yoon, Y.J., Lee, J.-I., Jang, Y.J., An, S., Kim, J.H., Fried, S.I., Im, M., 2020. Retinal degeneration reduces consistency of network-mediated responses arising in ganglion cells to electric stimulation. IEEE Trans. Neural Syst. Rehabil. Eng. 28, 1921–1930. https://doi.org/10.1109/TNSRE.2020.3003345.

Zaghloul, K.A., Boahen, K., Demb, J.B., 2003. Different circuits for ON and OFF retinal ganglion cells cause different contrast sensitivities. J. Neurosci. 23, 2645–2654. https://doi.org/10.1523/JNEUROSCI.23-07-02645.2003.

Zador, A., 1998. Impact of synaptic unreliability on the information transmitted by spiking neurons. J. Neurophysiol. 79, 1219–1229. https://doi.org/10.1152/jn.1998.79.3.1219.

Zrenner, E., Bartz-Schmidt, K., Gekeler, F., Greppmaier, U., Hekmat, A., Hoertdoerfer, G., Kernstock, C., Kitiratschiky, V., Sachs, H., Stingl, K., Wilhelm, B., 2012. Clinical study results with new wireless electronic subretinal implant alpha-ims. Acta Ophthalmol. 90. https://doi.org/10.1111/j.1755-3768.2012.4221.x, 0–0.